# A New Investigation of The Electronic Band Parameters for Cd$_{1-x}$Zn$_x$S Quantum Dot Superlattices

Nabil Safta

Unité de Physique Quantique, Faculté des Sciences, Université de Monastir, Avenue de l'nvironnement, 5000, Monastir – Tunisia

E-mail : *saftanabil@yahoo.fr*

***Abstract:*** This work reports on a theoretical investigation of superlattices based on Cd$_{1-x}$Zn$_x$S quantum dots embedded in an insulating material. These structures, assumed to a series of flattened cylindrical quantum dots with a finite barrier at the boundary, are studied using the Kronig – Penney method when the well width depends on the superlattice period. The fundamental miniband has been computed, for electrons, as a function of zinc composition for different inter-quantum dot separations. As is found, the fundamental miniband width decreases with the zinc composition and the superlattice period separately. Moreover, this study is of a great interest for designing novel nano devices, particularly, the nonvolatile memories.

***Keywords:*** Quantum dots, Superlattices, Cd$_{1-x}$Zn$_x$S, Kronig – Penney method, Nano devices

## I. INTRODUCTION

Films of Cd$_{1-x}$Zn$_x$S have attracted attention for a long time [1-10]. This is, essentially, related to the potentiality of Cd$_{1-x}$Zn$_x$S as a window material in hetero junction solar cells [5-6].

For quantum dots (QDs) based on the Cd$_{1-x}$Zn$_x$S ternary alloy, their interest has been exhibited in several fields [11-14]. For our part, we envisage, since several years, to use Cd$_{1-x}$Zn$_x$S QDs grown on nominal and vicinal Si surfaces [15-17] in order to promote novel nano devices such as the non - volatile memories. Thus, we can cite (i) our work made on the Cd$_{1-x}$Zn$_x$S QDs which considered the spherical geometry and an infinite potential model [18] (ii) our investigations based on the spherical geometry with a finite potential model [19-20]. However, the spherical geometry model is not commode to study the coupling between QDs. In order to around this difficulty, we have recommended the flattened cylindrical geometry with a finite potential model [21-33]. We have achieved several investigations concerning the electronic band parameters of super lattices based on Cd$_{1-x}$Zn$_x$S quantum dots inserted in a dielectric matrix [23-30]. In this context, our interest has been focused, in a previous study, on the calculation of the electronic band parameters with use the Kronig - Penney potential method [23]. It is worth to notice that in this study, the well width does not depend on the superlattice period and has a unique value for all the cases studied. Within this approximation, we have calculated the ground and the first excited minibands as well as the longitudinal effective mass for both electrons and holes.

The objective of the present work is to extend the last study in such a way that the well width depends on the superlattice period. The paper is presented as follows: after an introduction, we report an outline on the theoretical formulation and results. Conclusions are presented in the last section.

## II. MODELING

It is more realistic to use the spherical geometry in order to investigate the electronic properties    of Cd$_{1-x}$Zn$_x$S QDs embedded in a dielectric matrix. Figure 1- a shows the geometry used to describe a chain of Cd$_{1-x}$Zn$_x$S QDs. Nevertheless, along a common direction of spherical Cd$_{1-x}$Zn$_x$S QDs, one can

observe that electrons and holes see a succession of flattened cylinders of radius R and effective height L. With the assumption that L is lower than R, the quantum confinement along transversal directions can be ignored. Thus, the $Cd_{1-x}Zn_xS$ multi – quantum dot structure under study can be regarded as a QDs superlattice (SL) along the longitudinal confined direction denoted by z. For the $Cd_{1-x}Zn_xS$ QD superlattice, the $Cd_{1-x}Zn_xS$ flattened cylinders QDs correspond to wells whereas the host dielectric lattice behaves as a barrier of height $U_0$. The inter-QD separation, labeled as d, corresponds to the superlattice period. In addition, the electron and hole states are assumed to be uncorrelated. This approximation leads to a problem of one particle in a one-dimensional potential. In the present work, we suggest the Kronig - Penney potential (Figure 1- b). In this case, the electron and hole states can be calculated using the effective Hamiltonian:

$$H_{e,h} = \frac{-\hbar^2}{2m_{e,h}^*} \frac{d^2}{dz_{e,h}^2} + V(z_{e,h}) \qquad (1)$$

where the subscripts e and h refer to electrons and holes respectively, $m_{e,h}^*$ is the effective mass of carriers. In deriving the Hamiltonian $H_{e,h}$, we have considered the effective mass theory (EMT) and the band parabolicity approximation (BPA). The difference of the effective mass between the well and the barrier has been disregarded. The secular equation corresponding to the Hamiltonian $H_{e,h}$ is given by [23]:

For the bound states:

$$\cos k_{ze,h} d = ch\rho_{e,h}(d-L)\cos k_{e,h}L + \frac{1}{2}\left(\frac{\rho_{e,h}}{k_{e,h}} - \frac{k_{e,h}}{\rho_{e,h}}\right)sh\rho_{e,h}(d-L)\sin k_{e,h}L \qquad (2.a)$$

For the resonant states:

$$\cos k_{ze,h} d = \cos\eta_{e,h}(d-L)\cos k_{e,h}L - \frac{1}{2}\left(\frac{\eta_{e,h}}{k_{e,h}} + \frac{k_{e,h}}{\eta_{e,h}}\right)\sin\eta_{e,h}(d-L)\sin k_{e,h}L \qquad (2.b)$$

with, $k_{e,h} = \sqrt{\dfrac{2m_{e,h}^* E_{e,h}}{\hbar^2}}$

$$\rho_{e,h} = \sqrt{\frac{2m_{e,h}^*\left(U_{0e,h} - E_{e,h}\right)}{\hbar^2}} \quad \text{and} \quad \eta_{e,h} = \sqrt{\frac{2m_{e,h}^*\left(E_{e,h} - U_{0e,h}\right)}{\hbar^2}}$$

Where, $k_z$ is the wave vector parallel to the z direction and $E_{e,h}$ corresponds to the eigenenergies.

## III. RESULTS AND DISCUSSION

From Eqs (2-a) and (2-b), we have calculated, for electrons, the width $\Delta E_{1e}$ of the fundamental miniband ($\Gamma_{1e}$-miniband) in the case of $Cd_{1-x}Zn_xS$ QD structures. Values of parameters used in these calculations are taken from Ref [21] and listed in Table 1. Values of the electron effective masses for $Cd_{1-x}Zn_xS$ with different Zn compositions have been deduced using the linear interpolation. The well width L is considered as depending on the superlattice period d in such a way that $L = \frac{d}{10}$.
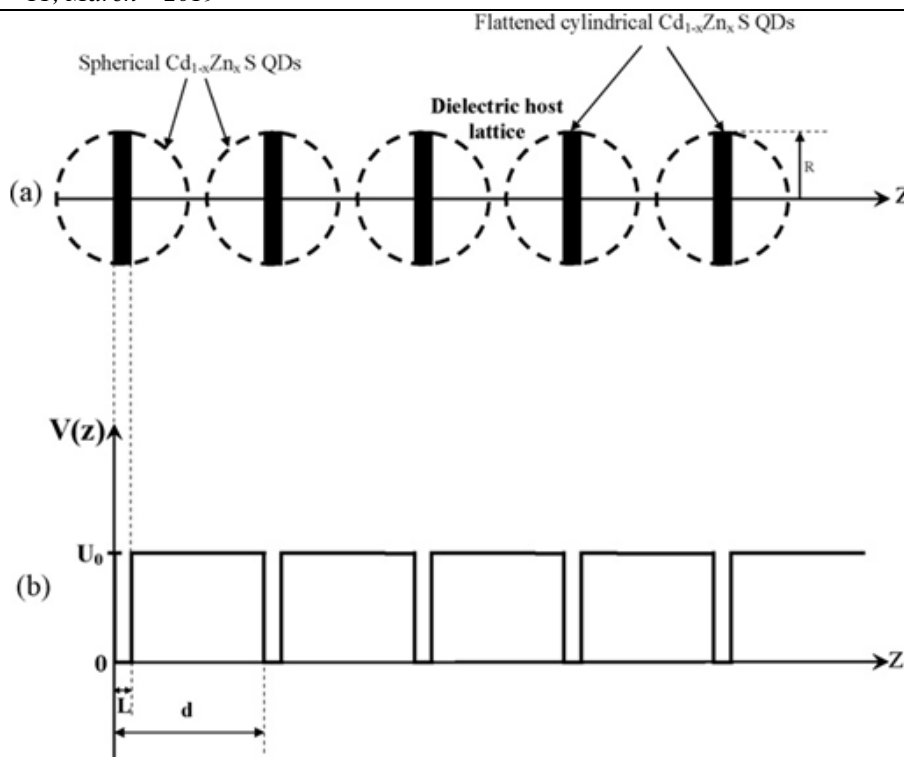
Figure-1(a): A schematic diagram of $Cd_{1-x}Zn_xS$ QD super lattices according to the flattened cylindrical geometry – (b) The barrier potential in the framework of the Kronig – Penney model.

Table 2 illustrates the obtained values of $\Delta E_{1e}$ as a function of zinc composition for different inter-quantum dot separations. It was revealed that, for any inter-QD separation, $\Delta E_{1e}$ decreases as a function of the Zn composition. This result is, only, due to the barrier potential height $U_{0e}$ which increases with x [21]. Indeed, the well width L is the same, for a given d value, and the effective mass $m_e^*$ remains practically unvaried for all Zn compositions. On the other hand, for any composition x, $\Delta E_{1e}$ decreases with the increase of the SL period d. The difference between the $\Gamma_{1e}$ - miniband widths for CdS QDs is equal to 0.66 eV while that of the ZnS-related QDs is of 0.36 eV. For intermediate compositions, this difference is located between the two extreme values.

Table 1. Parameters used to calculate the width $\Delta E_{1e}$ of the fundamental miniband for electrons in the case of $Cd_{1-x}Zn_xS$ QDs superlattices [21] ($m_0$ is the free electron mass)

| X | $\dfrac{m_e^*}{m_0}$ | $U_0(eV)$ |
|---|---|---|
| 0.0 | 0.16 | 0.10 |
| 0.2 | | 0.25 |
| 0.4 | | 0.45 |
| 0.6 | | 0.75 |
| 0.8 | | 1.50 |
| 1.0 | 0.28 | 2.00 |

Moreover, for $Cd_{1-x}Zn_xS$ QDs with low zinc compositions, the order of magnitude of the width $\Delta E_{1e}$ is important and shows a significant coupling between the QDs. This effect can induce metallic behavior in a dielectric host material.

At intermediate zinc compositions, $\Delta E_{1e}$ is lower and the coupling is, therefore, inferior. Concerning the high zinc compositions, $\Delta E_{1e}$ is extremely low. In the last case, $Cd_{1-x}Zn_xS$ QDs can be supposed as isolated.

Table 2. Widths of the $\Gamma_{1e}$- miniband (eV) for electrons in the case of $Cd_{1-x}Zn_xS$ QD superlattices

| d (nm)<br>x | 1.5 | 1.7 | 1.9 | 2.1 | 2.3 | 2.5 |
|---|---|---|---|---|---|---|
| 0.0 | 1.04 | 0.81 | 0.65 | 0.52 | 0.44 | 0.38 |
| 0.2 | 0.89 | 0.68 | 0.54 | 0.44 | 0.36 | 0.30 |
| 0.4 | 0.76 | 0.58 | 0.46 | 0.37 | 0.30 | 0.25 |
| 0.6 | 0.66 | 0.50 | 0.38 | 0.33 | 0.23 | 0.19 |
| 0.8 | 0.51 | 0.37 | 0.26 | 0.19 | 0.14 | 0.10 |
| 1.0 | 0.41 | 0.27 | 0.19 | 0.12 | 0.08 | 0.05 |

For comparison with results obtained by using the Kronig-Penney potential of the previous work [23], we report in Table 3, widths of $\Gamma_{1e}$- miniband as calculated in this work. As can be seen, the $\Gamma_{1e}$- miniband widths of the present work are higher for all the cases studied. This result can be explained in terms of the well width. Indeed, this parameter is inferior in the present work.

Table 3. Widths of the $\Gamma_{1e}$- miniband (eV) for electrons in the case of $Cd_{1-x}Zn_xS$ QD superlattices obtained in the previous work (L = 1 nm in all the cases studied) [23]

| d (nm)<br>x | 1.5 | 1.7 | 1.9 | 2.1 | 2.3 | 2.5 |
|---|---|---|---|---|---|---|
| 0.0 | 0.73 | 0.59 | 0.49 | 0.37 | 0.31 | 0.26 |
| 0.2 | 0.68 | 0.53 | 0.41 | 0.31 | 0.25 | 0.22 |
| 0.4 | 0.59 | 0.44 | 0.31 | 0.23 | 0.18 | 0.15 |
| 0.6 | 0.49 | 0.33 | 0.24 | 0.15 | 0.11 | 0.08 |
| 0.8 | 0.33 | 0.19 | 0.10 | 0.07 | 0.04 | 0.03 |
| 1.0 | 0.23 | 0.13 | 0.5 | 0.04 | 0.01 | 0.01 |

## IV. CONCLUSION

We investigated the electronic properties of superlattices based on $Cd_{1-x}Zn_xS$ embedded in a dielectric matrix. To describe the QDs, we have considered the flattened cylindrical geometry with a finite potential barrier at the boundary. Using the Kronig – Penney model when the well width is the tenth of the SL period, we have computed the ground miniband for electrons. Calculations have been effectuated as a function of Zn composition for different inter-quantum dot separations. An analysis of the results has showed that the $\Gamma_{1e}$- miniband width decreases with x and d separately. In addition, for $Cd_{1-x}Zn_xS$ QDs with low zinc compositions, the magnitude order of the fundamental miniband width is important and shows a significant coupling between the QDs. Moreover, the potential model adopted in the previous work does not account for the coupling as much as than the one of the present works.

In the applied physics, this study opens a new route for designing new devices based on $Cd_{1-x}Zn_xS$ QDs particularly the non – volatile memories.

**Conflict of interest:** The authors declare that the authors do not have any conflict of interest.

**Ethical statement:** The authors declare that they have followed ethical responsibilities.

## REFERENCES

[1]   A. Sakly, N. Safta and A. Ben Lamine (2004). Interpretation of the bowing phenomenon in $Cd_{1-x}Zn_xS$ alloy. J. Mater. Sci.-Mater. Electron, vol.15, p. 351.

[2]   N. A. Shah, A. Nazir, W. Mahmood, W. A. Syed, S. Butt, Z. Ali and A. Maqsood (2012). Physical properties and characterization of Ag doped CdS thin films. J. Alloys Compd, vol. 512, p. 27.

[3]   T.P. Kumar, S. Saravanakumar and K. Sankaranayanan (2011). Effect of annealing on the surface and band gap alignment of CdZnS thin films. Appl. Surf. Sci, vol. 257 (6), p. 1923.

[4]   B. Bhattacharjee, S. K. Mandal, K. Chakrabarti, D. Ganguli and S. Chaudhui (2002). Optical properties of Cd1−xZnxS nanocrystallites in sol–gel silica matrix. J. Phys. D: Appl. Phys, vol. 35, pp. 2636-2642.

[5]   H. H. Gürel, Ö. Akinci and H. Ünlü (2008). Tight binding modeling of CdSe/ZnS and CdZnS/CdS II–VI heterostructures for solar cells: Role of d-orbitals. Thin Solid Films, vol. 516, p. 7098.

[6]   M. Gunasekaram, M. Ichimura (2007). Photovoltaic cells based on pulsed electrochemically deposited SnS and photochemically deposited CdS and Cd1−xZnxS. Sol. Energy Mater. Sol. Cells, vol. 91, p. 774.

[7]   Z. Khéfacha, M. Mnari and M. Dachraoui (2002). Caractérisation des couches minces de Cd1–xZnxS préparées par dépôt chimique. Comptes Rendus Chimie, vol. 5(3), pp. 149-155.

[8]   Z. Khéfacha, Z. Benzarti, M. Mnari and M. Dachraoui (2004). Electrical and optical properties of $Cd_{1–x}ZnxS$ (0⩽x⩽0.18) grown by chemical bath deposition", Journal of crystal growth, vol. 260, pp. 400-409.

[9]   Z. Khéfacha, M. Mnari and M. Dachraoui (2003).  Opto – electronical of thin films prepared by chemical bath deposition. Physical and Chemical News. Vol.  14, pp. 77-84.

[10] S Alpdoğan, A O Adıgüzel, B Sahan, M Tunçer and H Metin Gubur (2017). Effects of bacteria on CdS thin films used in technological devices. Mater. Res. Express, vol. 4, p. 046402

[11] N.-K. Cho, J.-W. Yu, Y. H. Kim, and S. J. Kang (2014). Effect of oxygen plasma treatment on CdSe/CdZnS quantum-dot light-emitting diodes.  Jpn. J. Appl. Phys, vol. 53, p. 032101.

[12] Y. Wang, K. S. Leck, V. D. Ta, R. Chen, V. Nalla, Y. Gao, T. He, H. V. Demir, and H. Sun (2014). Blue liquid lasers from solution of CdZnS/ZnS ternary alloy quantum dots with quasi-continuous pumping. Adv. Mater, Doi: 10.1002/adma.201403237.

[13]  J. J. Beato-López, C. Fernández-Ponce, E. Blanco, C. Barrera-Solano, M. Ramírez-del-Solar, M. Domínguez, F. García-Cozar, and R. Litrán (2012). Preparation and characterization of fluorescent CdS quantum dots used for the direct detection of GST fusion proteins. Nanomaterials and Nanotechnology, vol. 2, p. 10.

[14] K. Deepa, S. Senthil, S. Shriprasad, and J. Madhavan (2014). CdS quantum dots sensitized solar cells. International Journal of Chem Tech Research, vol. 6, pp. 1956–1958.

[15] N. Safta, J-P. Lacharme and C.A.Sébenne (1993). Clean Si(110): a surface with intrinsic or extrinsic defects ?. Surf. Sci, vol. 287/288, pp.  312, 1993.

[16] N. Safta, J.P. Lacharme, A. Cricenti, A. Taleb-Ibrahimi,  Indlekofer, V.Aristov, C.A. Sébenne, G. Le Lay and B. Nesterenko (1995). Core level spectra of clean "2 × 8" vicinal Si (110). Nuclear Instruments and Methods in Physics Research B. vol. 97, p. 372.

[17] A. Cricenti, G. Le Lay, V. Yu Aristov, B. Nesterenko, N. Safta, J.P. Lacharme, C.A.  Sébenne, A. Taleb-Ibrahimi and G. Indlekofer (1995). High resolution syncrotron radiation Si 2p core-level spectroscopy of Si(110)16x2. Journal of Electron Spectroscopy and related phenomena, vol. 76,pp.  613-617.

[18]  Z. Khéfacha, N. Safta and M. Dachraoui (2016). The Band Gap Energy Calculated for  Cd1- xZnxS

Quantum Dots grown by the Sol gel Method.  International Journal of Applied Chemistry, vol.12, pp. 573-579.

[19]  N. Safta, A. Sakly, H. Mejri and Y. Bouazra (2006). Electronic and optical properties of $Cd_{1-x}Zn_xS$ nanocrystals.  Eur. Phys. J. B, vol. 51, pp. 75-78

[20]  A. Sakly, N. Safta, A. Mejri, H. Mejri, A. Ben Lamine (2010). The Excited Electronic States Calculated for Cd1-xZnxS Quantum Dots Grown by the Sol-Gel Technique. Journal of Nanomaterials 2010, Article ID 746520, 4 pages. doi:10.1155/2010/746520

[21] N. Safta, A. Sakly, H. Mejri and M. A. Zaïdi (2006). Electronic properties of multi-quantum dot structures in   $Cd_{1-x}Zn_xS$ alloy semiconductors. Eur. Phys. J. B, vol. 53, pp. 35 – 38.

[22] S. Marzougui, and N. Safta (2015). The excited electronic states and the oscillator strength calculated for flattened cylindrical Cd1-xZnxS quantum dots. International Journal of Chemistry and Materials Research, vol. 3, pp.17-26.

[23] A. Sakly, N. Safta, H. Mejri, A. Ben Lamine (2009). The electronic band parameters calculated by the Kronig–Penney method for $Cd_{1-x}ZnxS$ quantum dot superlattices. J. Alloys Compd, vol. 476, pp. 648–652.

[24] A. Sakly, N. Safta, H. Mejri, A. Ben Lamine (2011). The electronic states calculated using the sinusoidal potential for $Cd_{1-x}ZnxS$ quantum dot superlattices. J. Alloys Compd vol. 509, pp. 2493–2495.

[25] S. Marzougui, N. Safta (2014). The electronic band parameters calculated by the Triangular potential model for $Cd_{1-x}Zn_xS$ quantum dot superlattices. IOSR-JAP, vol. 5 (5), pp. 36-42.

[26]  S. Marzougui, N. Safta (2014). The electronic band parameters calculated by the Tight Binding Approximation for $Cd_{1-x}Zn_xS$ quantum dot superlattices.  IOSR-JAP, vol. 6 (2), pp. 15-21

[27] S. Marzougui, N. Safta (2014). A theoretical study of the electronic properties of$Cd_{1-x}Zn_xS$ quantum dot superlattices. American Journal of Nanoscience and Nanotechnology, vol. 2 (3), pp. 45-49.

[28] S. Marzougui and N. Safta (2014). A theoretical study of the heavy and light hole properties of Cd1-xZnxS quantum dot superlattices. International Journal  of Materials Science and Applications, Vol. 3, pp. 274-278.

[29] S. Marzougui and N. Safta (2015). The Electronic Band Parameters Calculated by a Novel Potential Model for Cd1-xZnxS Quantum Dot Super lattices. Research journal of Materials science, vol. 3, pp.  9-14.

[30] S. Marzougui and N. Safta, (2017). The Heavy and Light Hole properties studied by a Novel Potential Model for Cd1−xZnxS Quantum Dot Superlattices. International Journal of Advanced Engineering Research and Applications, Vol. 3, Issue. 7, pp. 263-269.

[31] S. Marzougui and N. Safta (2015). The electron transmission coefficient calculated for Cd1-xZnxS quantum dots-Application in the non volatile memories. International Journal of Applied Engineering Research, vol. 10 (21), pp. 42275-42278.

[32] Z. Khéfacha, N. Safta and M. Dachraoui (2017). The energy levels splitting calculated for electrons in a double $Cd_{1-x}Zn_xS$ quantum dot.  Journal of Advances in Nanomaterials, Vol. 2 (3), pp. 179-183.

[33] Z. Khéfacha, N. Safta and M. Dachraoui (2017). The Energy Levels Splitting Calculated for the Heavy and Light Holes  in a $Cd_{1-x}Zn_xS$ Double Quantum Dot. American Journal of Nano Research and Applications, vol. 5(3), pp. 32-36.

_____